Fire Technology, 52, 731–751, 2016
© 2015 Springer Science + Business Media New York.
Manufactured in The United States
DOI: 10.1007/s10694-015-0492-z

Experimental Procedures Characterising Firebrand Generation in Wildland Fires

Mohamad El Houssami, Eric Mueller, Jan C. Thomas and Albert Simeoni, BRE Centre for Fire Safety Engineering, The University of Edinburgh, Edinburgh EH9 3JL, UK*

Alexander Filkov, National Research Tomsk State University, Tomsk 634050, Russia

Nicholas Skowronski, Northern Research Station, USDA Forest Service, Morgantown, WV 26505, USA

Michael R. Gallagher and Kenneth Clark, Northern Research Station, USDA Forest Service, New Lisbon, NJ 08064, USA

Robert Kremens, Rochester Institute of Technology, Rochester, NY 14623, USA

Received: 26 September 2014/**Accepted:** 18 April 2015

Abstract. This study aims to develop a series of robust and efficient methodologies, which can be applied to understand and estimate firebrand generation and to evaluate firebrand showers close to a fire front. A field scale high intensity prescribed fire was conducted in the New Jersey Pine Barrens in March 2013. Vegetation was characterised with field and remotely sensed data, fire spread and intensity was characterised and meteorological conditions were monitored before and during the burn. Firebrands were collected from different locations in the forest and analysed for mass and size distribution. The majority were found to be bark slices (more than 70%) with substantial amounts of pine and shrub twigs. Shrub layer consumption was evaluated to supplement the firebrand generation study. Bark consumption was studied by measuring the circumference variation at several heights on each of three different pine trees. The variation was in the same order of magnitude as the bark thickness (1–5 mm). Testing and improving the protocol can facilitate the collection of compatible data in a wide range of ecosystems and fire environments, aiding in the development of solutions to prevent structural ignition at the Wildland Urban Interface.

Keywords: Firebrands, Generation, Pine forest

1. Introduction

Wildland fires have a dramatic impact on human life, property, and the environment. They cause significant economic losses, as demonstrated by the devastating wildfires that occurred over the last few years. In 2014, more than 63,000 wildland fires burned over 1.4 million hectares in the United States [1]. In 2013, a total of 2135 structures were destroyed by these wildfires, including 1093 residences, 945

* Correspondence should be addressed to: Mohamad El Houssami, E-mail: m.elhoussami@ed.ac.uk

out-buildings and 97 commercial structures [1]. The problem of spreading wildfires causing the ignition of houses and buildings is not new, with thousands of properties destroyed every year. The impact of these fires is expected to increase dramatically [2] with the rapid expansion of the Wildland Urban Interface (WUI) [3, 4] and because changing climate will likely increase the occurrence and intensity of forest fires [5]. The main factors that influence structural ignition in the WUI are heat transfer from approaching flames (radiation and convection) and the deposition of firebrands that can accumulate on the outer surface of a home or find a way through the structure to reach easy-to-ignite fuels or structural elements [6]. The intense exposure to firebrands in the vicinity of a fire front is called firebrand shower and it is the main condition of exposure from firebrands at the WUI [7]. Firebrand generation is the process through which wildland fuels, such as shrubs and trees are heated and broken into smaller burning pieces during a fire, and transported away from the fire through the plume [8], creating spot fires [9]. For more than 40 years, most studies have focused on understanding how far firebrands can fly [10–13], and fewer studies have evaluated their production at field scale [7].

Woycheese et al. [14] conducted firebrand combustion tests in wind tunnel in various flow conditions on disc-shaped firebrands of different species and sizes. These experiments provided mass, volume and density history curves. Seven species of wood were tested and the effects of diameter and length-to-diameter ratio were examined in relative velocities ranging from 1 m s^{-1} to 7 m s^{-1}. Over the years, samples were collected from different incidents and were studied. In the 1991 Oakland Hills conflagration, a firebrand was found 1 km away from the fire, which had ~5 mm thickness, ~50 mm diameter and 2.3 g, presumed to be produced for cedar shingle [8]. More recently, Manzello et al. [7] examined the size distribution and other characteristics of firebrand exposure during the WUI Angora fire in California in 2007 by measuring the hole size from trampolines that were exposed to firebrands during a fire. Similarly, in Texas the same technique was used following the Bastrop Complex Fire in 2011 [15], which was the most destructive fire in Texas history, and the third most destructive in the history of the United States.

Multiple laboratory experiments were conducted to study flaming and glowing firebrands on pine needle beds, shredded paper beds and other materials [16, 17]. Firebrands were deposited on fuel beds, and the diameter of the firebrands in the rage of 25 and 50 mm. Under light winds of 0.5 to 1 m s^{-1}, both flaming and glowing firebrands had the ability to initiate spot fires. Other laboratory experiments determined the size and mass distribution of firebrands generated from a single Douglas-fir tree [18]. It was found that the firebrands were cylindrical shapes with an average size of 3 mm in diameter, 40 mm in length for 2.6 m trees and 4 mm in diameter with a length of 53 mm for 5.2 m trees. It should be noted that these experiments were conducted in still air and that all the particles falling from the trees were collected. As mentioned in the study by Koo et al. [8], bigger trees were observed to produce bigger firebrands. Vodvarka et al. [19] made the same observation for firebrands produced by structure fires. Additionally, a firebrand generator [20] was developed at the National Institute of Standards and

Technology to generate a controlled and repeatable size and mass distribution of glowing firebrands. This apparatus was used in different situations such as testing the vulnerability of roofing materials to firebrand attacks [21]. Finally, Koo et al. [8] recommend that firebrand generation research should focus on the rate of firebrand produced in the main fire. On that account and beyond the results reported here, this work aims to develop a protocol for characterising firebrand generation in terms of particle mass, particle size and origin in the field on relation to fire properties and more particularly, fire intensity. This study focused on firebrand showers created in the vicinity of a fire front, and not on long distance spotting. It does not cover the contribution of firebrands to fire propagation either.

2. Approach

2.1. Site Description

The study was conducted in the Pinelands National Reserve (PNR) in southern New Jersey (USA) in March 2013. The PNR is the largest forested landscape on the North-eastern coastal plain, and covers 23% of New Jersey. The execution of a larger project [22] on the effect of fuel treatments on fire spread rate and intensity afforded the opportunity to study firebrand production on this site. Fuels were already characterised, both by field sampling and by airborne Light Detection and Ranging (LiDAR) calibrated with ground measurements [23]. The ambient temperature was around 7°C, and mean relative humidity was 39%. The stand was approximately 6 hectares, dominated by Pitch pine (Pinus rigida Mill.) and scattered oaks (*Quercus* spp.). Understory vegetation consisted of scrub oaks, huckleberry (*Gaylussacia* spp.) and blueberry (*Vaccinium* spp.).

2.1.1. Fire Characterisation Approach A network of four instrumented meteorological towers in the overstory and twelve towers in the understory was established at the burn site. Three 12.5 m overstory towers were located within the burn block, and the fourth was located upwind in an adjacent stand. Instrumentation included sonic anemometers at the top of each tower providing high frequency (10 Hz) measurements of three wind speed components located at 12.5 m. At the control tower, additional instrumentation was used to measure wind speed and direction, air temperature, relative humidity, atmospheric pressure, and soil temperature in order to measure ambient conditions during the fire [22]. Sonic anemometers were oriented with their horizontal axes aligned in the east–west and north–south (true north) directions. This allowed for a characterisation of the three-dimensional turbulence regimes before, during, and after the passage of the fire fronts through the tower locations. Multi-spectral airborne imagery was prepared using Rochester Institute of Technology's Wildfire Airborne Sensor Program (WASP) [24], in order to track the fire progression in both visual and three distinct infrared (IR) bands (short-wave, mid-wave, and long-wave). Pre- and post-fire canopy fuel loadings were estimated using an airborne LiDAR model allowing the generation of a 1 m × 1 m resolution canopy height profile [23], as well as 3D canopy bulk density (CBD) at a resolution of 10 m × 10 m × 1 m. 1.

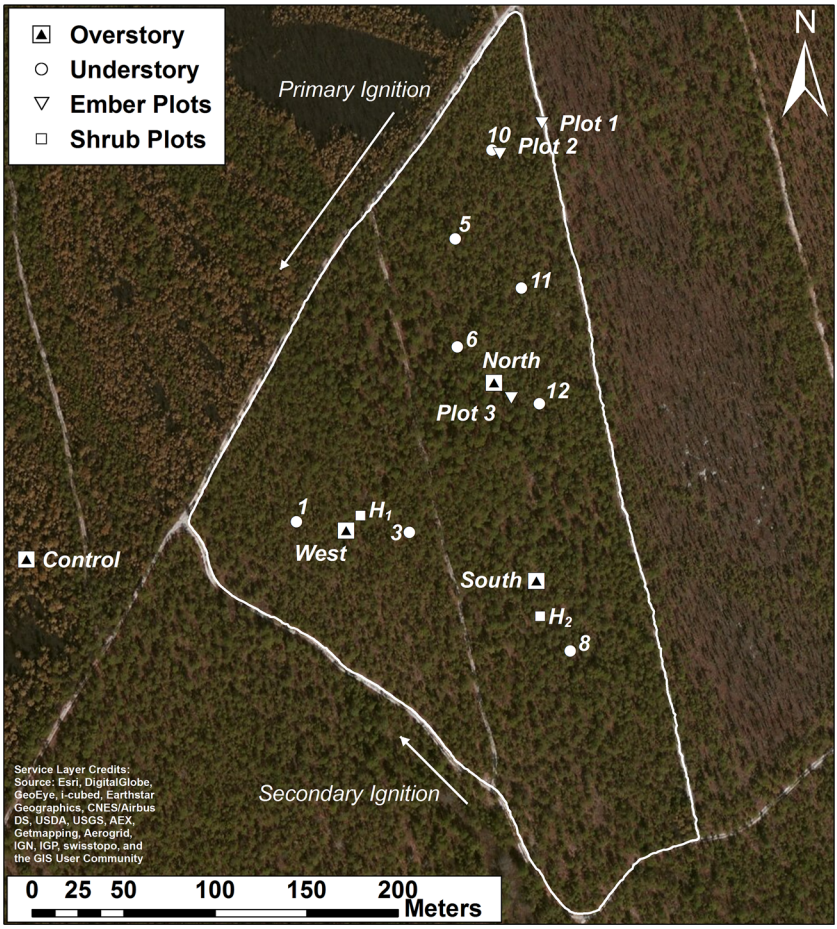

Figure 1. Selected important locations in the field.

Airborne LiDAR data was calibrated to provide estimates of canopy bulk density, through the combined use of an upward-sensing terrestrial LiDAR and destructive field sampling, following in the methodology of Clark et al. [25]. Additionally, a number of digital and analogue cameras were placed throughout the block. These cameras were intended to record characteristics of the fire, such as flame heights. A simplified overview of the instrumentation location is presented in Figure 1.

2.2. Firebrand Study

2.2.1. Shrub Layer Measurements In addition to the clip plot sampling for the canopy fuel loadings, a methodology was developed and tested to characterise shrub layer fuel consumption at a finer scale than typically considered. While 1-h fuels are defined as having a diameter $<6.35 \times 10^{-3}$ m [26], it is desirable for the study to determine the size of consumed particles at a higher resolution and to link it to firebrand generation. Therefore, 1 h fuels were divided into sub-groups:

– S_1: <2.00 × 10^{-3} m;
– S_2: 2.01 to 4.00 × 10^{-3} m;
– S_3: 4.01 to 6.35 × 10^{-3} m.

Current methods involve destructive fuel sampling before and after the fire. An alternative method with several advantages is proposed here:

– Detailed subcategories,
– Easy to implement (fast, one person job),
– Non-destructive,
– Allows fuel consumption visualisation.

Two sample plots (H_1, H_2) were randomly selected within the burn unit to characterise the shrub layer (Figure 1). Series of pictures were taken in front of a white background, which was used to enhance the contrast per sample site. One sample shrub was selected for more detailed inspection, measuring stem and branch diameters with a precision calliper. These measurements were used for quantification of live particle size consumed in the fire.

2.2.2. Pine Bark Measurements Section measurements were made on three different pine trees to estimate the variations in tree sections before and after the fire. These measurements were then used to calculate the reduction of bark thickness due to the fire. Several sets of 8 nails were placed along the circumference at different heights (Figure 2, points 1 to 8) and the angle between consecutive nails was 45° ± 10°. A flexible measuring tape (±5 × 10^{-4} m precision) was used to measure S_n, the distance between two consecutive nails at each height, both before and after the fire. Knowing this, a radius can be calculated for each section. The difference between 2 radii (ΔR_n) measured pre and post fire can indicate the bark thickness that was lost from the tree.

$$\forall n \in [1,8] \quad \Delta R_n = R_n - R'_n = \frac{4(S_n - S'_n)}{\pi} \tag{1}$$

2.2.3. Firebrand Collection The firebrand collection was inspired by the method used in [27, 28] and applied on a larger scale. Fire resistant gypsum boards were placed on the ground at three sites. 20 aluminium pans, 0.3 × 0.24 m each were positioned on each board to form a rectangle with a total cross section area of 1.4 m^2. Wire nets were placed inside the pans to allow easy extraction of captured firebrands. Pans were filled with water to extinguish falling burning particles. Plot 1 was placed near the track, delimiting the experimental parcel (Figure 1), Plot 2 and Plot 3 were placed near measuring towers. In Plot 2 only, pans were covered by a thin plastic film. Laboratory experiments showed that holes burnt in the film allowed the location and approximate size of falling particles to be determined, and allowed particles that had sufficient energy to make their way through the

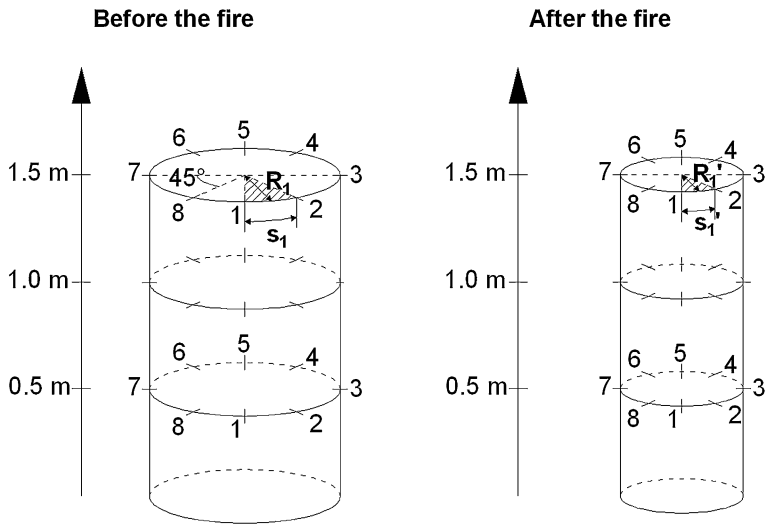

Figure 2. Illustration of trunk measurements.

film to be determined. The collected firebrands in this plot either passed through the film, or were found stuck to it. This means that the collected particles were burning (by flaming or smouldering) and were not cold particles breaking away from vegetation after the fire front was gone.

3. Results and Discussion

3.1. Fire Behaviour and Impact

The average horizontal wind, measured at 12.5 m, was 1.8 m s^{-1} with gust values of 6.4 m s^{-1}. These values are considered as low wind compared to more severe wildland fire conditions in the same ecosystem [29], and compared to a study that was conducted in the same Pine Barrens and had active crowning conditions [30]. It took place in the years immediately following the Warren Grove wildfire and was burning in decimated forest conditions where there was no risk of escape. It is therefore impossible to obtain such extreme conditions on a regular basis for experimental fires. Despite the high peak values reported in the previous study, the average wind speed for the period examined was 3.0 m/s.

Figure 3 displays seven front lines derived from the WASP (fire contours P2 to P8). These fire contour lines were obtained from the pixel intensity recorded in the long-wave (8.0 to 9.2 μm) infrared spectral band for sequential passes of the associated aircraft. For each pass, the gradient of pixel intensity was calculated, and dereferenced contour lines were hand-traced along the steepest gradient using ArcGIS. ROS were calculated in the areas of interest near the firebrand plots (hatched). The primary fire front originated from the northwest road, along the primary ignition line, and then spread in a south-easterly direction.

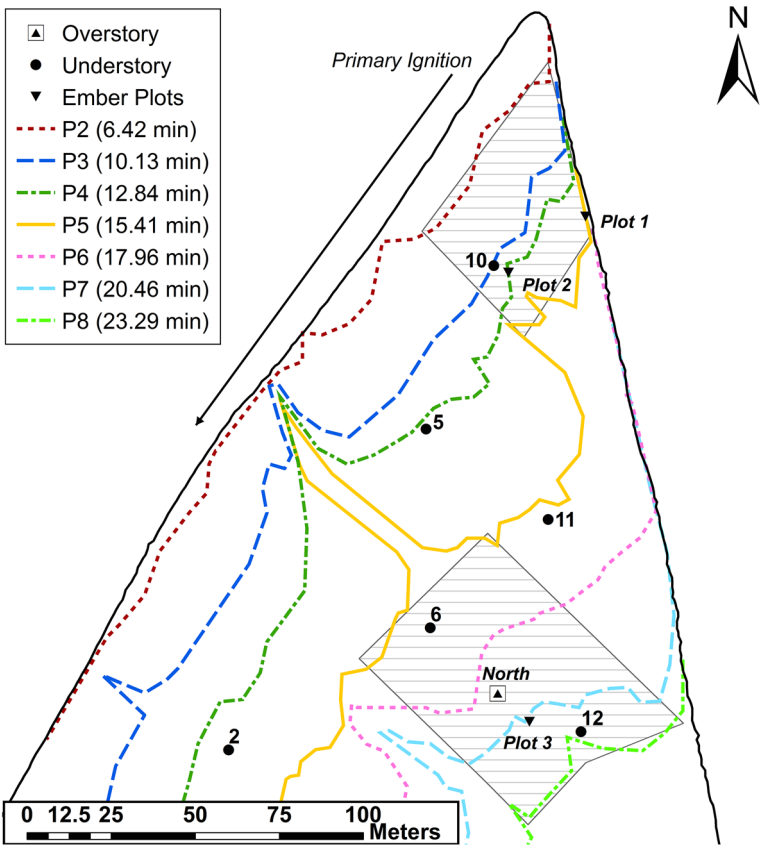

Figure 3. Fire front progression with consecutive fire contours (P2 to P8). Time of each contour is given in minutes after ignition.

During the burn, it was observed that the fire mainly spread in the shrub layer in the section of the block in which the ember collection took place. The absence of continuous crown fire can also be confirmed by the examination of video footage. Figure 4a shows one frame of footage close to the east road looking in the direction of Understory 11 (U_{11}) (Figure 3), which was located in the region where the ember collection study occurred. Figure 4b shows one frame footage of firebrands flying across a fuel break and igniting the other side.

Fire line intensity is important for characterising the type of fire observed, which is meant to indicate the energy release rate per unit length of fire front [31]. Fireline intensity is often calculated as:

$$I = H \times \Delta m \times ROS \tag{2}$$

ROS is the rate of spread [m s^{-1}] determined from IR imagery. Δm is the mass of fuel consumed [kg m^{-2}], and H is the heat yield of the fuel. In this study, H is

Figure 4. (a) Snapshot looking in the direction of Tower 11 during the burn; (b) Snapshot of firebrands flying across a fuel break.

18,700 kJ kg^{-1} [32]. Currently, only fine fuel (primarily needle litter), 1 h forest floor wood, and 1 h oak and shrub layer material were used to calculate the fireline intensity. This is because these small fuels are dominant contributors and because consumption measurements for larger fuel classes are less reliable. Hence, it is referred to as surface fireline intensity (I_{surf}). Interpolated values of Δm, ROS, and their corresponding I_{surf} values are presented in Table 1 for each understory

Table 1
Summary of Mass fuel Consumption, Percentage of Initial Mass Consumed, Rate of Spread and Surface Fireline Intensity

Location	Δm (kg m^{-2})	% Δm	Distance	ROS (m s^{-1})	I_{surf} (kW m^{-1})
Understory 10	0.73 ± 41%	56	P2–P3	0.095 ± 11%	1300 ± 42%
			P2–P4	0.074 ± 10%	1000 ± 42%
			P2–P5	0.073 ± 9%	1000 ± 42%
			P3–P4	0.039 ± 36%	500 ± 55%
			P3–P5	0.055 ± 28%	700 ± 50%
			P4–P5	0.074 ± 49%	1000 ± 64%
Understory 6	0.93 ± 36%	64	P5–P6	0.186 ± 18%	3200 ± 40%
			P5–P7	0.180 ± 18%	3100 ± 40%
			P6–P7	0.161 ± 35%	2800 ± 50%
Understory 12	0.64 ± 26%	62	P6–P7	0.161 ± 35%	1900 ± 44%
			P6–P8	0.137 ± 15%	1600 ± 30%
			P7–P8	0.101 ± 30%	1200 ± 40%

tower location. The towers of interest are Understory 6, 10 and 12 denoted U_6, U_{10}, and U_{12} respectively.

U_{10} near the start of the ignition line experienced the lowest intensities with values ranging between 500 kW m^{-1} and 1300 kW m^{-1}, resulting from low mass consumption and low rate of spread. Then, the fire intensity increases while propagating to U_6, then to U_{12} with values ranging between 1600 kW m^{-1} and 3200 kW m^{-1}. Surface fireline intensities can be compared to other shrubland fires, such as those summarised in [33]. The estimates given here also relate only to surface fire intensity, and do not consider any canopy fuel consumption which occurred. However, an examination of this canopy consumption is very important for assessing fire behaviour. Although quantitative values of biomass consumed are not used in this study, a qualitative analysis of percent canopy consumption can provide valuable information. The percent difference in the pre- and post-fire canopy bulk density [kg m^{-3}] was obtained along transects following the direction of fire spread and passing through grid cells containing understory towers and plots of interest. In this case, canopy bulk density was estimated using models which only considered available fuels (defined as live and dead needles, live and dead 1 h fuels, and dead 10 h fuels [25]). The results are shown in Figure 5. It should be noted that the scale of Figure 5 does not reflect the fact that some negative values of consumption were found. Near the ignition line, this was determined to be the result of a systematic error in the Airborne Laser Scanning (ALS) data which degraded the quality of measurements made in isolated areas. Efforts are being made to correct this issue in the data, however, the general trends shown in Figure 5 follow observations made in the field. Several other negative values found along the transect in Figure 5b were found to be small in magnitude, reaching the limit of the current measurement capabilities. Additionally, due to the uncertainty that is associated with classifying LiDAR returns into ground and non-ground points in systems with high shrub loading, we do not consider the height bin between 0 m and 1 m here.

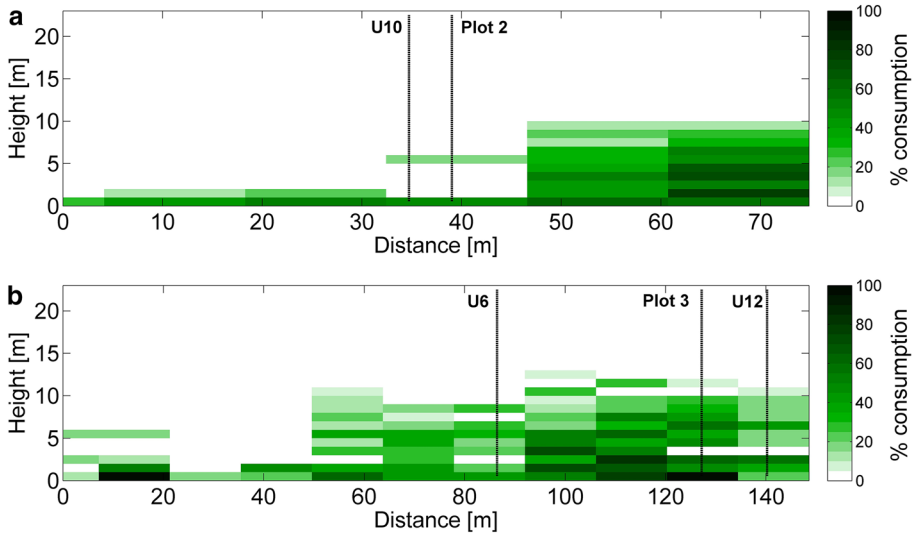

Figure 5. Percent of available canopy fuels consumed as estimated from LiDAR data. Transects are shown in direction of fire spread for (a) Understory 10 and Plot 2, (b) Understory 6 and 12, and Plot 3. Distance is given in meters from ignition line.

A comparison of the transects reveals that U_{10} and Plot 2 had relatively little canopy fuel consumption, corresponding to the lower surface fireline intensities. In both cases, as the fire reached roughly 40 to 60 m from the ignition line, a transition to partial canopy fuel consumption occurred. Referring to Table 1, this transition from U_{10} to U_6 is reflected in the fact that surface fireline intensity nearly doubled as the fire passed through this region. This type of canopy fuel involvement continued as the fire spread from U_6 to U_{12}, surrounding Plot 3. Additional fire behaviour results and analysis are the subject of ongoing work [34]. During the burn, it was observed that the fire mainly spread in the shrub layer in the section of the block in which the ember collection took place. Post-fire observations in the area revealed that tree crowns in many areas had been largely unaffected. However, intermittent torching into tree crowns was observed, as well as a region of more substantial crown consumption close to U_{11}. An example of the surface fire behaviour can be found by the examination of video footage (Figure 4a and 4b).

3.2. Firebrand Study

3.2.1. Shrub Layer Consumption After the burn, each site was revisited, the background placed in the same location and pictures taken. Pre and post fire pictures from sample shrubs in each plot were analysed to determine which branches were consumed. Fire intensities at shrub sites H_1 was in the same range as U_6 (Table 1) but it was difficult to assess it at H_2 as it was located near the intersection of fronts spreading in opposite directions. In the pre and post fire picture (Figure 6)

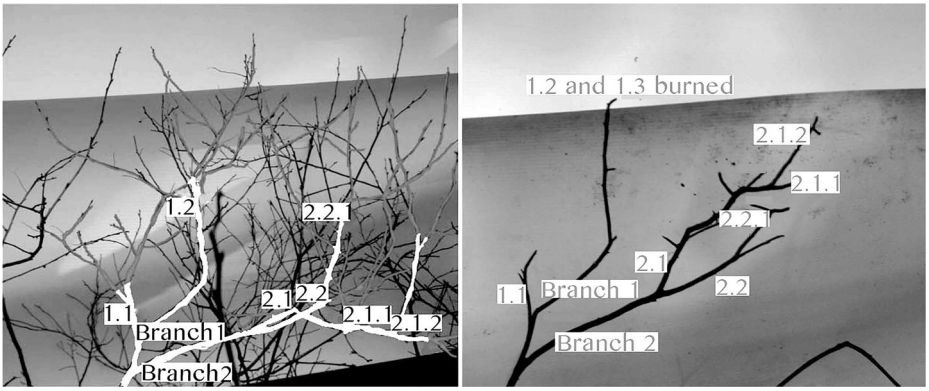

Figure 6. Sampled shrub, pre and post fire.

Table 2
Branch Diameter of Sample Shrub in Site H_1 ($\times 10^{-3}$ m)

			Stem 8.65		
	Branch 1 4.91			Branch 2 6.55	
*Branch 1.1** *3.19*	**Branch 1.2** **2.05**	**Branch 1.3*** **2.20**	Branch 2.1* 5.07		Branch 2.2* 2.95
			*Branch 2.1.1** *2.54*	*Branch 2.1.2** *3.7*	*Branch 2.2.1* *2.54*

In normal: only charred, in bold: totally burned, in italic: partially burned

each branch at the sample shrub is labelled for visibility. The highlighted branches indicate which portion of the shrub was still present after the fire. Only few branches were left after the fire.

Table 2 shows the diameter of each branch. For clarification: Branch 1 had three branches originating from it, hence these are labelled branch 1.1, 1.2 and 1.3. Branches smaller than 2×10^{-3} m were consumed, as it was predicted that all branches in this range are consumed. The (*) indicates that the branch has further branches that were less than 2×10^{-3} m. No comparison between pre and post fire measurements was done because the main interest was to track what disappeared and not the diameter regression.

It is clear from the pictures and branch diameter measurements that not all 1 h fuels were consumed by the fire. Hence, it is important to determine sub classes as described above. 100% of S_1 particles were consumed. S_2 particles were partially consumed, and S_3 particles were not consumed. At first estimation, if it is considering that 50% of S_2 particles burned, one could conclude that not more than 53% of 1 h fuel was consumed in the fire (Equation 3).

Table 3
Percentage of Total Mass for Different Group Size

Sub-group	Size ($\times 10^3$ m)	Percent of total mass (dry) (%)
S1	<2.00	32
S2	2.01 to 4.00	42
S3	4.01 to 6.35	26

$$\text{Consumption} = (X_{S1} \times 100\%) + (X_{S2} \times 50\%) + (X_{S3} \times 0\%) = 53\% \quad (3)$$

With X representing the mass fraction of each subgroup (Table 3). If computer models assume 100%, then it is clear that this is not a valid assumption. A very similar scenario was found at sample site H_2. These results have implication on fire modelling and will provide further insight on where to focus efforts in the future. In summary, despite the fact that the fuel and the fire are very dependent, sub-groups dividing 1-h fuel particles into smaller categories should be established because not all 1-h particles contribute to the fire evenly. Furthermore, fuel moisture content will be characterised based on these subclasses, which will play a role in the fuel consumption. These preliminary results indicate that we do not fully understand the dynamics of particle consumption within the shrub layer. However, there is a need to perform this experiment with more attention to statistical design so that the results can be properly characterised and tested.

In addition to the non-destructive sampling, a large collection of huckleberry samples (0.75 kg) was collected from various locations within the block. The shrubs were cut at the base, and entire shrubs were analysed in the laboratory. This sampling was done to get a sense of the proportions of the shrub mass, which fall into each subgroup of 1 h fuel (Table 3). Besides the stem, most branches of the huckleberry shrub fell into the 1 h fuel class.

3.2.2. Pine Bark Consumption Tree boles were clearly affected during surface fires regardless of the height (up to 3 m). Figure 7 shows a one-frame footage of a tree bole burning and pieces of bark detaching from the tree, 1 min after the fire front has passed. This picture clearly shows that the fire-induced draft is an important parameter for bark originated firebrand production and transport. Therefore it is necessary to quantify this production. It is also important to note that the bark could delaminate or expand due to heat. Hence, the measured variations can be overestimated due the neglected expansion. In order to compare these variations, the radius variations were calculated as explained earlier and are distributed for different size ranges in Figure 8. The error margin from the conversion from circumference to radius is 3.2×10^{-4} m. The distribution shows that a few millimetres in depth of the bark were consumed during the fire. Most of the measurements are between 0.32 and 4×10^{-3} m then can go up to 1.4×10^{-2} m.

3.2.3. Firebrand Collection The collected firebrands were dried at 80°C in an oven until reaching a constant weight, then weighed on a laboratory balance with a

Figure 7. Footage bark pieces burning and detaching from the tree.

precision of 0.1 mg, taking into account only particles with a mass greater than 5 mg. Particle dimensions (length, width, and thickness) were measured using an electronic caliper ($\pm 10^{-5}$ m). 5 particles were measured 10 times and the systematic measurement error (difference between the mean value and maximum or minimum value) was no more than 6%. Particles smaller than 5×10^{-3} m were discarded. Figure 9 shows firebrand samples collected from the experiment, Figure 10 shows photographs of Plots 2 and 3, respectively after the fire.

It was found that 70 to 89% of particles were bark slices and the rest were branches. About 30% of all firebrands had a mass between 10 mg and 20 mg and few of them more than 100 mg. The following distribution is found when branch-originated firebrands are separated from bark fragments (Figure 11):

All of the collected firebrands ranged between 1 mm and 6 mm in thickness. Most of the branches were between 2 and 6×10^{-3} m and very few were less than 2×10^{-3} m in diameter, which means that the latter are consumed before reaching the collecting pans. Whereas most of bark firebrands were in 1 to 2×10^{-3} m range but can go up to 6×10^{-3} m. These values are in the same order of magnitude as the bark thickness collected in the pans (Figure 8). Therefore, this study

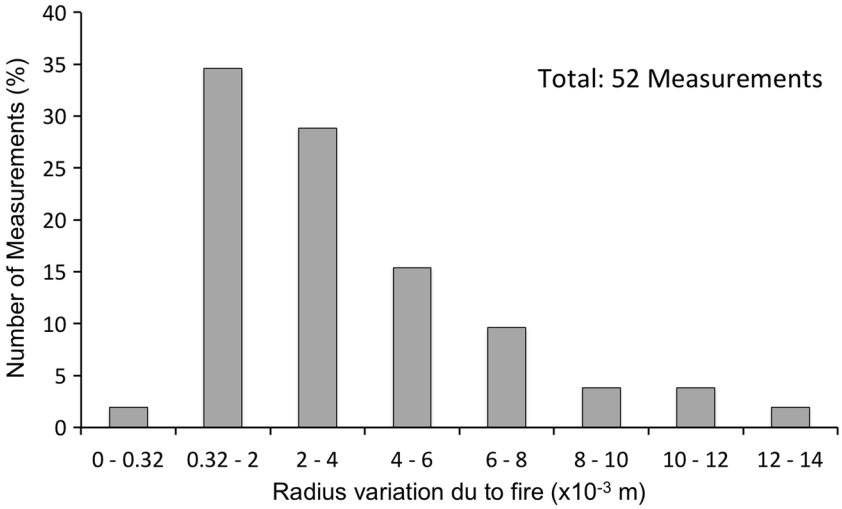

Figure 8. Radius variation due to the fire ($\pm 3.2 \times 10^{-4}$ m).

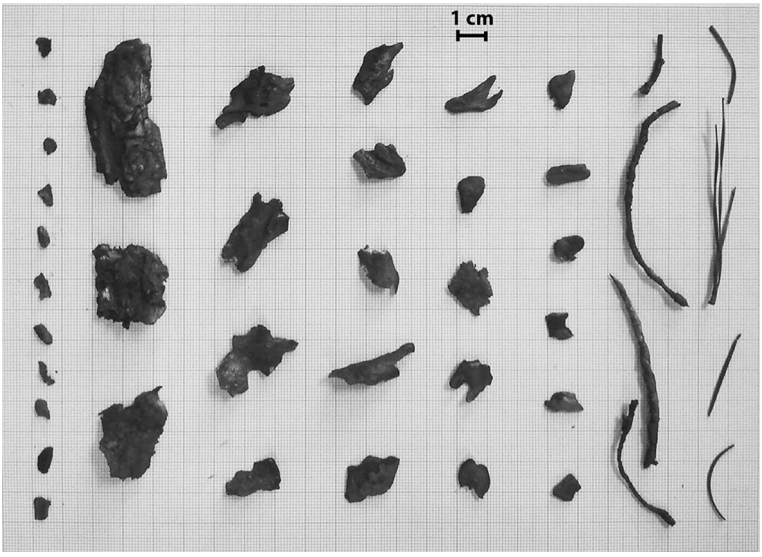

Figure 9. Firebrand samples.

proves that bark slices from pine trees participate in firebrand generation. Figure 10 can be reorganised using the S sub-groups, giving the distribution in Figure 12:

The totality of S_1 particles was consumed but very few were found in the pans, which mean that they burn very fast. S_2 particles contributes the most in the firebrand generation since more than 70% are found in the pans, it is therefore easy

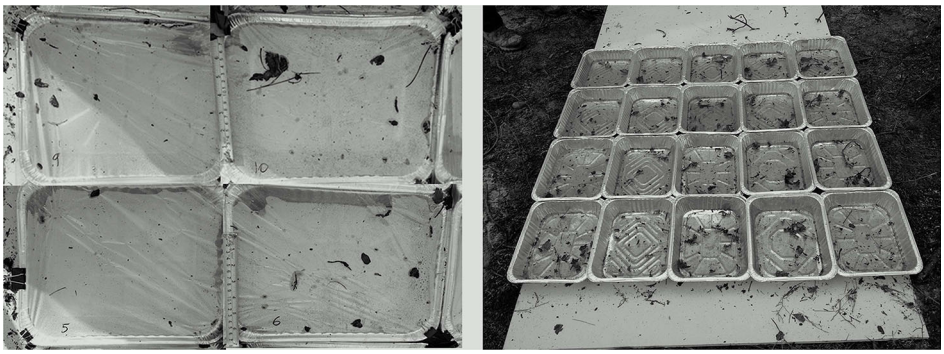

Figure 10. Plots 2 and 3 after the fire.

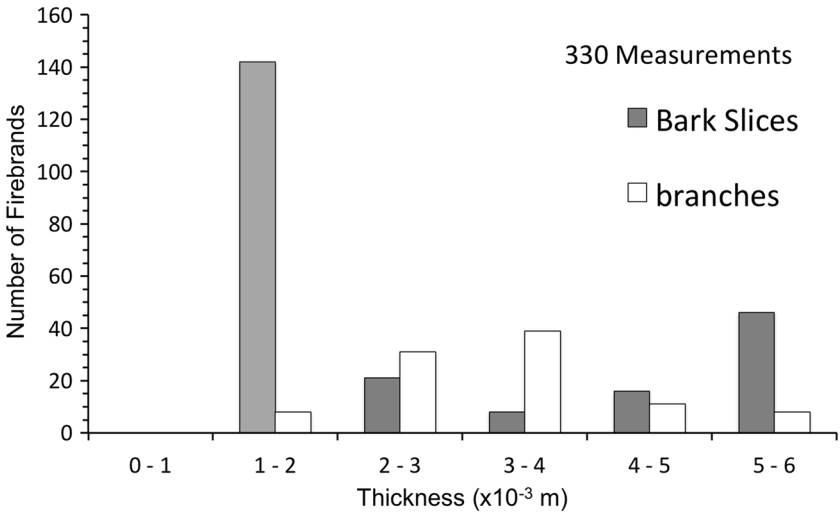

Figure 11. Separated firebrand distribution by size ($\pm 10^{-5}$ m, 330 measurements).

to ignite, can be transported easily and burns for enough time to reach a target. S_3 particles are less likely to ignite since none of the measurements show that they were consumed. The mass and area for each particle was also measured and a distribution for the three plots is shown in Figures 13 and 14. The majority of firebrands weighed between 5 mg and 20 mg, and only a few particles were found to exceed 100 mg. A size analysis of firebrands shows that the majority (45 to 63%) were particles with a cross section area of 0 to 10×10^{-5} m^2. Cross section areas are estimated by considering bark pieces as rectangles and shrubs as cylinders. About 80% of all particles had a cross section area in the range of 0 to 20×10^{-5} m^2. These findings are in agreement with the case study findings of the Angora fire [7] where more than 85% of holes that firebrands had made on trampolines

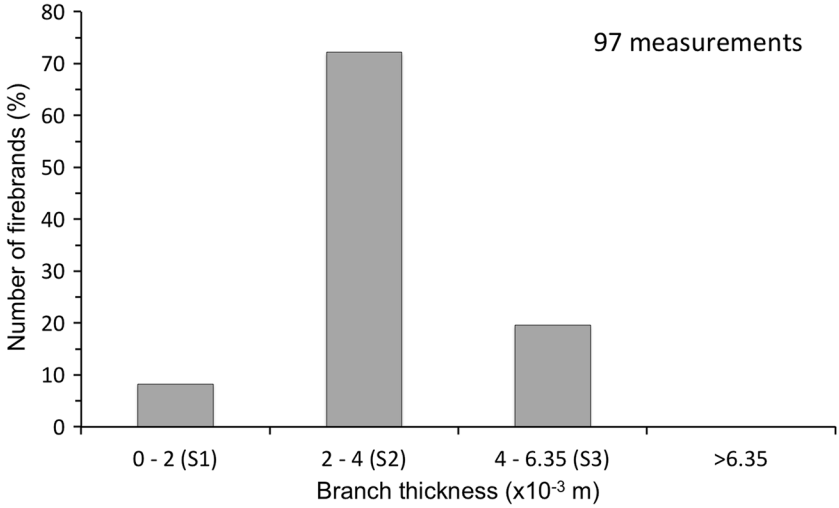

Figure 12. Branch-originated firebrand distribution using sub-groups ($\pm 10^{-5}$ m).

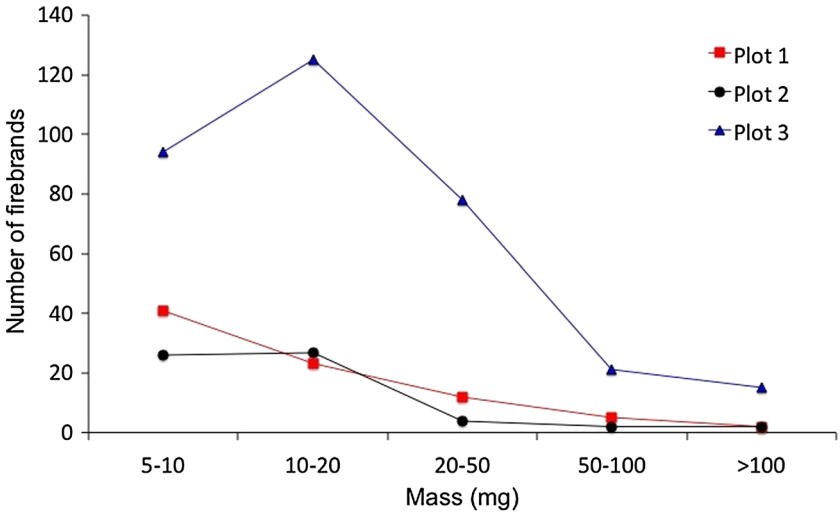

Figure 13. Firebrand distribution by mass for each plot ($\pm$0.1 mg).

were measured at less than 0.05 cm^2 (50 $\times$ 10^{-5} m^2). Similarly, another case-study in Texas [15] observed more than 90% of the holes made in trampolines that were smaller than 0.5 cm^2 (5 $\times$ 10^{-5} m^2). The quantity of collected firebrands over the pan array surface provides a firebrand density (Table 4).

Plot 1 (without film) and Plot 2 (with film) have similar results; Plot 1 was near the track (Figure 1), hence was less exposed to the fire front and remotely re-

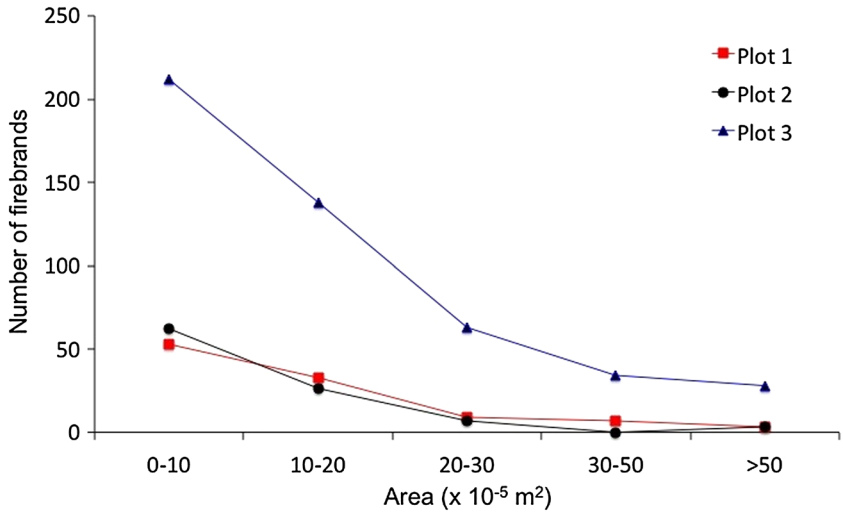

Figure 14. Firebrand distribution for different area ranges.

Table 4
Quantity of Collected Firebrands (>5 mg and >5 × 10^{-3} m) in Each Plot and Its Corresponding Density

Location	Quantity	Density (m^{-2})
Plot 1	83	60
Plot 2	61	44
Plot 3	333	238

ceived firebrands during the fire, and not after. Plot 2 was more exposed to the fire, but the film was able to separate firebrands from cold particles falling from the trees after the fire. It is observed that plot 3 (without film) contained about 6 times more particles than plot 1 and 2. As presented in Figure 5b, Plot 3 was located in a more intense surface fire with burning involved in the canopy. A difference is seen in quantity of particles only for small and light ones. This suggests that a greater proportion of small particles may have fallen in Plot 3 than in Plot 1 and 2 after the fire. The use of a plastic film is essential to separate cold particles from burning ones. But it was also observed that many small burning particles were not able to enter the collecting pans because of the plastic film. A solution would be to position the plots closer to the track, on a fuel break, at a certain distance from the fireline and from any trees, without plastic film cover. This way, only firebrands will be collected. This situation also represents a real scenario where a structure is exposed to a burning forest at a known distance.

Through these experiments, it is found that 1 h fuel is not fully consumed in the same way at short ranges. A portion is participating in the firebrand generation before being consumed. This portion contains pieces of shrubs but is largely dominated by bark pieces, which is probably due to the cylindrical shape of shrub

branches, that doesn't allow them to be transported easily opposed to bark originated firebrands.

4. Conclusion

A study on the generation of firebrands was carried out during a prescribed burn in the Pinelands National Reserve of southern New Jersey. The fire was observed to be a plume dominated surface fire within the section of the block pertaining to this study. Ambient wind conditions were relatively low. ROS and fire intensity was determined using WASP, revealing that ROS was comparable to other shrub fires [33]. However, surface fire intensity was found to be much lower (10 times), due to a lower fuel loading. Fuel consumption in the canopy was determined qualitatively using the LiDAR technique. Transects showed the different fire regimes in the selected areas: a low intensity fire was involved ahead of Plot 1 and 2, whereas more canopy fuel was consumed ahead of Plot 3. Consistent with the goal of this work, three different methodologies were explored in order to examine the firebrands produced at different locations of this fire. Several interesting preliminary findings were obtained. The shrub layer consumption was evaluated in order to supplement the firebrand generation study. The methodology applied utilised pre and post fire photographs and branch size measurements to estimate the consumption. It was found that 1 h fuels should be divided into sub-groups (S_1, S_2, and S_3) because not all 1 h fuel was consumed. Very few S_1 particles were found in the collection pans, which means that these are mostly consumed immediately, or before reaching a target. Most branch particles (70%) found in the pans are of type S_2. Therefore, it suggests that these particles are not fully consumed by the fire and are the major component of firebrands. S_2 particles are easy to ignite, light enough to be transported and hold enough energy to continue burning until reaching a target. S_3 particles are less likely to ignite since none of the measurements show that they were consumed. The technique was found to be an easy and inexpensive procedure that produces more insight into the consumption of small particles. More measurements are needed throughout the parcel to quantify the consumption depending on the heterogeneity of the fuel and the variation of fire behaviour.

Three pine trees were randomly selected for measurements in the forest. The trunk surface was consumed from the ground to more than 2 m even though there was no crowning in the areas selected. The bark consumption was determined by measuring the circumference/radius regression of each tree at different heights. Most of the radius variations were between 0.32 and 4×10^{-3} m (with a maximum value of 14×10^{-3} m), which are in the same order of magnitude as the particle bark thickness collected in the pans. This study will allow estimating the generation quantitatively per tree during a surface fire with further study if more measurements are added in order to become statistically significant. More detailed characterisation of the fire intensity and residence time near the tree will be needed for further studies.

The quantity and characteristics (mass, size) of firebrands generated by the fire on 3 plots were determined. It was found that most particles (70 to 89%) were bark slices. About 30% of all firebrands had a mass between 10 mg and 20 mg and few of them were more than 0.1 g. About 80% of all particles were in the range of 0–20 $\times$ 10^{-5} m^2. The thickness of firebrands did not exceed 6 $\times$ 10^{-3} m. The number of firebrands decreased with increasing firebrand area. Many small burning particles were not captured in the pans because of the plastic film. A better solution would be to position the plots outside of the burning area, on a fuel break and to collect firebrands without any cover.

This work represents a first exploration of various methodologies. Some of the most important results came in the form of gained experience and the enlightenment of potential improvements to the aforementioned techniques. Other conditions will be tested, to establish correlation between fire behaviour, fuel consumption and firebrand generation and to obtain more statistically significant data. The current findings show that even for controlled fire in low wind conditions, firebrands are still produced at short range and were quantified. These results can be used as threshold for simulation purposes and for laboratory scale experiments, in which different fuel species can be test under the same conditions.

Acknowledgments

Authors thank the New Jersey Forest Fire Service. The field experiment was supported by the Joint Fire Science Program (Project 12-1-03-11). Dr. Filkov was supported by the Fulbright program of Institute of International Education, the Government Assignment in the Field of Scientific Activity (Number 1624) and by the President of the Russian Federation Scholarship (Number SP-3968.2013.1).

References

1. National Interagency Coordination Center (2013) Wildland Fire Summary and Statistics, Annual Report. http://www.nifc.gov/fireInfo/nfn.htm
2. Foote EID, Liu J, Manzello SL (2011) Characterizing firebrand exposure during wildland urban interface fires. Proceedings of Fire and Materials Conference
3. Maranghides A, Mell W (2013) Framework for Addressing the National Wildland Urban Interface Fire Problem - Determining Fire and Ember Exposure Zones Using a WUI Hazard Scale.
4. Hammer RB, Radeloff VC, Fried JS, Stewart SI (2007) Wildland-urban interface housing growth during the 1990s in California, Oregon, and Washington. International Journal of Wildland Fire 16:255–265
5. Flannigan MD, Stocks BJ, Wotton BM (2000) Climate change and forest fires. Sci Total Environ 262:221–229
6. Cohen JD (2000) What is the wildland fire threat to homes? In: Thompson Memorial Lecture, April 10, 2000 School of Forestry, Northern Arizona University, Flagstaff, AZ. http://www.fs.fed.us/rm/pubs_other/rmrs_2000_cohen_j003.pdf

7. Manzello SL, Foote EID (2014) Characterizing Firebrand Exposure from Wildland-Urban Interface (WUI) Fires: Results from the 2007 Angora Fire. Fire Technol 50:105–124. doi:10.1007/s10694-012-0295-4
8. Koo E, Pagni PJ, Weise DR, Woycheese JP (2010) Firebrands and spotting ignition in large-scale fires. International Journal of Wildland Fire 19:818–843
9. Viegas DX, Almeida M, Raposo J et al (2014) Ignition of Mediterranean Fuel Beds by Several Types of Firebrands. Fire Technol 50:61–77. doi:10.1007/s10694-012-0267-8
10. Tarifa CS, DelNotario PP, Moreno FG (1965) On the flight paths and lifetimes of burning particles of wood. Tenth International Symposium on Combustion. The Combustion Institute, Cambridge, UK, pp. 102–1037
11. Albini FA (1979) Spot fire distance from burning trees–a predictive model. General Technical Report INT-56 73p
12. Albini FA (1983) Transport of Firebrands by Line Thermals. Combust Sci Technol 32:277–288
13. Tse SD, Fernandez-Pello AC (1998) On the flight paths of metal particles and embers generated by power lines in high winds - a potential source of wildland fires. Fire Saf J 30:333–356
14. Woycheese J. (2000) Brand lofting and propagation from large-scale fires. PhD thesis. University of California – Berkeley
15. Rissel S, Ridenour K (2013) Ember Production During the Bastrop Complex Fire. Fire Mananagement Today 72:
16. Manzello SL, Cleary TG, Shields JR, Yang JC (2006) Ignition of mulch and grasses by firebrands in wildlandurban interface fires. International Journal of Wildland Fire 15:427–431. doi:10.1071/WF06031
17. Manzello SL, Cleary TG, Shields JR, Yang JC (2006) On the ignition of fuel beds by firebrands. Fire Mater 30:77–87. doi:10.1002/fam.901
18. Manzello SL, Maranghides A, Mell WE (2007) Firebrand generation from burning vegetation. International Journal of Wildland Fire 16:458–462. doi:10.1071/WF06079
19. Vodvarka V (1969) Firebrand field studies – Final report. Report no. IITRI-J6148. Chicago
20. Manzello SL, Shields JR, Cleary TG et al (2008) On the development and characterization of a firebrand generator. Fire Saf J 43:258–268
21. Manzello SL, Suzuki S, Hayashi Y (2012) Enabling the study of structure vulnerabilities to ignition from wind driven firebrand showers: A summary of experimental results. Fire Saf J 54:181–196
22. Mueller E, Skowronski N, Simeoni A, et al. (2013) Fuel Treatment Effectiveness in Reducing Wildfire Intensity and Spread Rate – An Experimental Review. 4th Fire Behavior and Fuels Conference
23. Skowronski NS, Clark KL, Duveneck M, Hom J (2011) Three-dimensional canopy fuel loading predicted using upward and downward sensing LiDAR systems. Remote Sens Environ 115:703–714. doi:10.1016/j.rse.2010.10.012
24. McKeown D, Faulring J, Krzaczek R, et al. (2011) Demonstration of delivery of orthoimagery in real time for local emergency response. In: Shen SS, Lewis PE (eds) Algorithms and Technologies for Multispectral, Hyperspectral, and Ultraspectral Imagery XVII. p 80480G–80480G–11
25. Clark K, Skowronski N, Gallagher M, et al. (2013) Assessment of Canopy Fuel Loading Across a Heterogeneous Landscape Using LiDAR
26. Johnson EA, Miyanishi K (2001) Forest Fires. Academic Press, San Diego, pp. 585–594

27. Manzello SL, Cleary TG, Shields JR et al (2008) Experimental investigation of firebrands: generation and ignition of fuel beds. Fire Saf J 43:226–233
28. Suzuki S, Manzello SL, Lage M, Laing G (2012) Firebrand generation data obtained from a full-scale structure burn. International Journal of Wildland Fire 21:961. doi:10.1071/WF11133
29. Hughes JB (1987) New Jersey, April 1963: Can it happen again?. Fire Management Notes 48:3–6
30. Manzello SL, Park S-H, Cleary TG (2010) Development of rapidly deployable instrumentation packages for data acquisition in wildland–urban interface (WUI) fires. Fire Saf J 45:327–336. doi:10.1016/j.firesaf.2010.06.005
31. Byram GM (1959) Combustion of forest fuels. In: Davis, K.P., ed. Forest fire: control and use. New York McGraw Hill 61–89
32. Alexander ME (1982) Erratum: Calculating and interpreting forest fire intensities. Can J Bot 60:2185–2185. doi:10.1139/b82-267
33. Morandini F, Silvani X (2010) Experimental Investigation of the Physical Mechanisms Governing the Spread of Fire. International Journal of Wildland Fire 19:570–582
34. Mueller E, Skowronski N, Clark K, et al. (2014) An experimental approach to the evaluation of prescribed fire behavior. Advances in forest fire research. doi: http://dx.doi.org/10.14195/978-989-26-0884-6_4